Original Article

Automatic Choroidal Segmentation in Optical Coherence Tomography Images Based on Curvelet Transform and Graph Theory

Reza Alizadeh Eghtedar[1], Mahdad Esmaeili[1], Alireza Peyman[4,5], Mohammadreza Akhlaghi[4,5], Seyed Hossein Rasta[1,2,3]

[1]Medical Bioengineering Department, School of Advanced Medical Sciences, Tabriz University of Medical Sciences, Tabriz, Iran, [2]Department of Medical Physics, School of Medicine, Tabriz University of Medical Sciences, Tabriz, Iran, [3]Department of Biomedical Physics, School of Medical Sciences, University of Aberdeen, Aberdeen, UK, [4]Department of Ophthalmology, Isfahan University of Medical Sciences, Isfahan, Iran, [5]Isfahan Eye Research Center, Department of Ophthalmology, Isfahan University of Medical Sciences, Isfahan, Iran

Abstract

Background: Automatic segmentation of the choroid on optical coherence tomography (OCT) images helps ophthalmologists in diagnosing eye pathologies. Compared to manual segmentations, it is faster and is not affected by human errors. The presence of the large speckle noise in the OCT images limits the automatic segmentation and interpretation of them. To solve this problem, a new curvelet transform-based K-SVD method is proposed in this study. Furthermore, the dataset was manually segmented by a retinal ophthalmologist to draw a comparison with the proposed automatic segmentation technique. **Methods:** In this study, curvelet transform-based K-SVD dictionary learning and Lucy-Richardson algorithm were used to remove the speckle noise from OCT images. The Outer/Inner Choroidal Boundaries (O/ICB) were determined utilizing graph theory. The area between ICB and outer choroidal boundary was considered as the choroidal region. **Results:** The proposed method was evaluated on our dataset and the average dice similarity coefficient (DSC) was calculated to be 92.14% ± 3.30% between automatic and manual segmented regions. Moreover, by applying the latest presented open-source algorithm by Mazzaferri *et al*. on our dataset, the mean DSC was calculated to be 55.75% ± 14.54%. **Conclusions:** A significant similarity was observed between automatic and manual segmentations. Automatic segmentation of the choroidal layer could be also utilized in large-scale quantitative studies of the choroid.

Keywords: *Choroidal segmentation, curvelet transform, graph theory, image processing, optical coherence tomography*

Submitted: 04-Aug-2021 **Revised:** 25-Apr-2022 **Accepted:** 10-Jun-2022 **Published:** 29-May-2023

Introduction

The choroid layer (the region between the outer choroidal boundary [OCB] and the inner choroidal boundary [ICB]) is a vascular structure in the posterior part of the eye between the sclera and retina and possesses some key roles in the eyes including oxygen supply and feeding of the retina [Figure 1]. Several parameters such as age and some eye diseases affect the thickness of choroid.[1-4]

Optical coherence tomography (OCT) is a novel noninvasive imaging technique, which is applied to the imaging of the human retina.[5] The enhanced depth imaging OCT (EDI-OCT) obtains high-resolution cross-sectional images of the choroid and has been used in recent works on choroidal segmentation.[6]

The main objective of automatic choroidal segmentation is to help ophthalmologists to monitor and diagnose eye diseases. This fact has made many researchers, all around the world, to focus on the subject. Most ophthalmologists segment this layer using manual or semi-automatic techniques. The inhomogeneous intensity of the choroidal layer, low contrast of OCT images, and the presence of speckle noise have made automatic choroidal segmentation to be a challenging task.[7,8] To reduce speckle noise from OCT images, many traditional methods such as adaptive median and Wiener filtering,[9,10] median, and Lee filtering[11-14] are suggested but these methods are often obscure in details and affect edges in an image. In this paper, we have used a new 2-dimensional (2D) curvelet-based K-SVD algorithm[15] to speckle noise reduction. Even though this method enhances intraretinal layers, with noise suppression and optimally despeckling OCT image, the texture preservation (TP)

How to cite this article: Eghtedar RA, Esmaeili M, Peyman A, Akhlaghi M, Rasta SH. Automatic choroidal segmentation in optical coherence tomography images based on curvelet transform and graph theory. J Med Signals Sens 2023;13:92-100.

Address for correspondence:
Dr. Seyed Hossein Rasta, Department of Medical Bioengineering, Faculty of Advanced Medical Sciences, Tabriz University of Medical Sciences, Tabriz 51666, Iran.
E-mail: s.h.rasta@abdn.ac.uk

Access this article online

Website: www.jmssjournal.net

DOI: 10.4103/jmss.jmss_144_21

Quick Response Code:

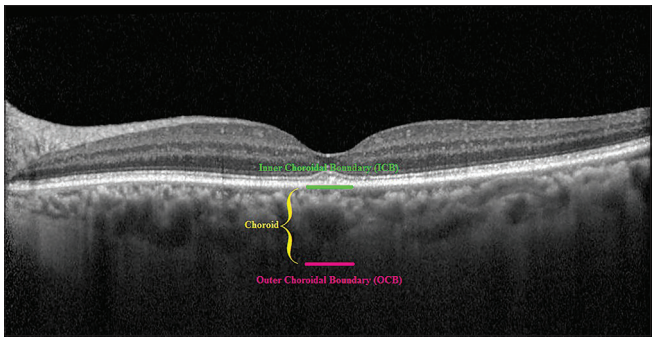

Figure 1: A sample of an EDI-OCT image of the choroid. EDI-OCT - Enhanced depth imaging-Optical coherence tomography; ICB - Inner choroidal boundaries; OCB - Outer choroidal boundaries

parameter, which is a measure of retaining texture in a region of interest (ROI), seems not to be satisfactory (TP would be close to 0 for severely flattened image and remains close to 1 at its best). Therefore, to correct these weaknesses and deblurring of the resulting images, we used an efficient Lucy–Richardson deconvolution algorithm[16] to enhance intra-retinal boundaries and deblur the resulting images. Furthermore, we introduced a new method based on graph theory and curvelet transform, for automatic segmentation of the choroid in OCT images. The experimental results showed that automated extracted regions significantly matched with the manual segmentations helped the ophthalmologists in recognizing eye abnormalities.[17] Table 1 shows the reported Dice Coefficient in other studies and introduces them briefly.

Nowadays, much work has been done in the field of automatic segmentation of OCT images, therefore, a brief review of automatic choroidal segmentation methods is included here. Vedran Kajić *et al*.[18] used a neural network, machine learning using stochastic modeling, convex hull, Dijkstra's shortest path, and active appearance model on spectral domain OCT (SD-OCT) images of 12 adult eyes. Torzicky *et al*.[19] used depolarization and the birefringence of the sclera, on polarization sensitive OCT images of five healthy subjects. To this end, Tian *et al*.[20] proposed a gradient-based graph search method on EDI-OCT images of 45 healthy adults. Zhang *et al*.[21] utilized a graph-based multilayer segmentation method on 3-dimensional (3D) SD OCT (3D SD-OCT) images of 24 normal subjects. Hu *et al*.[22] proposed a gradient-based multistage graph search algorithm on SD-OCT images of 20 eyes from 20 healthy and 10 eyes from 10 nonneovascular age-related macular degeneration (AMD) adults. Lee *et al*.[23] used the 3D graph-cut method in EDI-OCT images of eyes with nonneovascular AMD. Lu *et al*.[24] presented a gradient-based graph search on OCT images of 30 adult subjects suffering from diabetes. David Alonso-Caneiro *et al*.[7] used edge filter, directional weight, dual brightness probability gradient, and the Dijkstra's shortest path algorithm on EDI-OCT images of 1083 pediatric B-scans and 90 adult B-scans. Danesh *et al*.[5] used the largest gradient, dynamic programming, Gaussian mixture model, and wavelet features in EDI-OCTs of 6 healthy adult subjects. Gerendas *et al*.[25] proposed an Iowa reference algorithm on SD-OCT images of 142 patients with Diabetic Macular Edema. Srinath *et al*.[26] used adaptive Hessian analysis on OCT images of the posterior part of the eyes. Vupparaboina *et al*.[27] used tensor voting, structural similarity index, and Eigen value analysis of the Hessian matrix on SD-OCT images of 5 healthy adult participants. Chen *et al*.[28] proposed gradual intensity distance, thresholding, graph min-cut max-flow, and the energy minimization methods on SD-OCT images of 66 patients. Shi *et al*.[29] utilized a 3D graph search method on OCT images of 32 normal eyes. Twa *et al*.[30] presented dynamic programming, graph theory, and wavelet-based texture analysis technique on SD-OCT images of 30 young adult subjects. Sui *et al*.[31] used graph-edge weights learned from deep convolutional neural networks on OCT images of 42 normal subjects and 31 patients with macular edema. Chen *et al*.[32] proposed a 3D graph search method on 3D SD-OCT images of 41eyes. Mazzaferri *et al*.[17] utilized a graph-based method on SD-OCT images of 280 patients. Al-Bander *et al*.[33] presented a deep learning algorithm on 169 EDI-OCT images. Chen *et al*.[34] used convolutional neural networks on 62 EDI-OCT images of patients with AMD. Wang *et al*.[35] proposed the Markov random field, 3D nonlinear anisotropic diffusion filter, and level set techniques on 3D OCT images of 30 healthy subjects. Hussain *et al*.[36] presented Dijkstra's shortest path algorithm on EDI-OCT images of 10 subjects. Furthermore, Salafian *et al*.[37] used Dijkstra's algorithm in the neutrosophic space on 32 EDI-OCT images of 11 subjects. Masood *et al*.[8] utilized deep learning techniques and morphological operations on OCT images of 21 individuals. George and Jiji[38] presented multi-level contour evolution based on the Chan-Vese algorithm while the dataset was the same with Danesh *et al*.[5] Furthermore, a complete and detailed description of the latest relative automatic choroidal segmentation methods is presented in the study by Alizadeh Eghtedar *et al*.[39]

The challenging issues associated with automatic choroidal segmentation in OCT images include the depth of choroidal tissue, the vascular and heterogeneous structure of this layer makes recognition of the layer difficult task.[7] In this study, we try to cope with the mentioned challenges and present a new and fully-automated technique for the segmentation of the choroid in EDI-OCT images. To prevent inaccurate detection of choroidal boundaries, at first, the OCT images are preprocessed and the reflective layers above the Bruch's membrane are removed, then the curvelet transform is used and curvelet coefficients are modified to enhance and fill the black shadowing effects. The graph-based segmentation of ICB and OCB layers may be degraded

Table 1: Graph-based segmentation methods of the choroidal region in optical coherence tomography images

Author and year	Dataset and samples	Denoising and preprocessing algorithm	Segmentation method	Results
Tian *et al*., 2012[18]	45 B-scan from 45 healthy adult subjects	Wiener filter and N-point moving average	Gradient-based graph search and dynamic programming	Mean dice coefficient=90.5%±3%
Zhang *et al*., 2012[19]	24 normal subjects were imaged twice on the same day	A three-stage approach to change the contrast of the silhouette regions	Graph-based method.	Dice coefficient=78%±8%
Lu *et al*., 2013[20]	30 adult subjects with diabetes	Not mentioned	Gradient-based graph search, and dynamic programming	Mean dice coefficient=92.7%±3.6%
Alonso-Caneiro *et al*., 2013[7]	90 adult B-scans from 15 healthy subjects and 1083 pediatric B-scans from 104 healthy subjects	A coarse average filter with a rectangular size of 5×22 pixels, to smooth the image	Dijkstra's shortest path algorithm, directional weight, Edge filter, dual brightness probability gradient	Mean dice coefficient=96.7%±2.1%
Vupparaboina *et al*., 2015[21]	97 B-scans per eye, from 5 healthy adult subjects	The BM3D algorithm	Tensor voting, structural similarity index, and eigenvalue analysis of the Hessian matrix	Mean dice coefficient=95.47%±1.73%
Shi *et al*., 2016[22]	32 normal eyes	Linear mapping and a cross bilateral filtering	3D graph search method with the gradient-based cost	Mean dice coefficient=93.17%±1.30%
Al-Bander *et al*., 2017[23]	169 EDI-OCT images	The intensity values given closer to the sclera were multiplied with the cumulative sum, to increase the contrast of the ROI	Deep learning algorithm (CNN)	Dice coefficient=89.76%
Chen *et al*., 2017[24]	62 EDI-OCT images of patients with age-related macular degeneration	Not mentioned	CNN	Mean dice coefficient=82%±1%
Wang *et al*., 2017[25]	30 images from 30 healthy subjects with the ages between 20 to 85 years	Conventional anisotropic diffusion approach	Markov random field and level set methods	Mean dice coefficient=90%±4%
Masood *et al*., 2019[8]	525°CT images (25 scans from every 21 subjects)	Reconstruction approach based on the morphological opening	Deep learning and a series of morphological operations	Mean dice coefficient=97.35%±2.3%

EDI – Enhanced depth imaging; 3D – Three dimensional; OCT – Optical coherence tomography; BM3D – Block-matching and 3D filtering; ROI – Region of interest; CNN – Convolutional neural networks

because of the presence of these possible gaps due to large vessels.

This article is organized as follows: section 2 explains the algorithm used for denoising and enhancement of OCT images and automatic segmentation of choroidal thickness. Section 3 presents the used dataset and compares the performance of the manual segmentations versus the segmentations done with the proposed method and segmentations done with the method proposed by Mazzaferri *et al*.,[17] also the comparison of choroidal segmentation of original images and the denoised images using the proposed method is given in this section. Finally, the paper discusses in section 4 and concluding points are given in section 5.

Materials and Methods

Preprocessing and denoising

Un-preprocessed OCT images, like ultrasound images, do not have smooth appearances because of the presence of speckle noise that pollutes image features. By denoising OCT images, images quality can be improved leading to an accurate analysis of intra-retinal layers including the choroidal layer. In other words, removing speckle noise and contrast enhancement in the OCT images corrects the structural heterogeneity in the OCB area, thus, the preprocessing step improves the choroidal segmentation. In this study, a 2D curvelet-based K-SVD algorithm[12] was used to the speckle-noise reduction of OCT images. The dictionary size was 16 × 256 for the coefficient matrix on scale 7 and was 16 × 128 used for denoising the curvelet coefficient matrix on scale 6. Although this method has acceptable performance, the TP parameter was not satisfactory and the resulting images suffered from blurring effects, thus, an effective Lucy–Richardson's deconvolution algorithm[13] was used to enhance and deblur the resulting images.

Lucy–Richardson's deconvolution algorithm was originated from the theorem of Bayes by Lucy and Richardson in the 1970s.[40,41] Among the various deconvolution algorithms been investigated in different studies, Lucy–Richardson has been reported to be

the algorithm with the most prosperous results.[16,42,43] This algorithm is commonly used due to its ability in recovering blurred and noisy images, which have been blurred by a known point spread function (PSF).[16] The main formula of the algorithm is as follows:[16]

$$g_{n+1}(x, y) = g_n(x, y)\left[u(-x, -y) \otimes \frac{k(x, y)}{u(x, y) \otimes g_n(x, y)}\right] \quad (1)$$

Where:

$g_n(x, y)$ is the undistorted image estimation in the n^{th} iteration. The process of enhancement starts with $g_0(x, y) = k(x, y)$ and improves $g_n(x, y)$ based on the original output image $k(x, y)$, and $u(x, y)$ is the PSF of the imaging system, Figure 2 shows the block diagram of the proposed method for OCT image despeckling.

Segmentation of inner choroidal boundaries and outer choroidal boundary

In this study, an automatic algorithm, based on Dijkstra's shortest path graph-search algorithm, that was fully described in following references,[44,45] is used to segment the ICB. Each pixel of the OCT image corresponds to a graph node and the link between two adjacent nodes is characterized by a weight value. By calculating the lowest weight between any two nodes on the entire graph the preferred path between them is determined by Dijkstra's algorithm.[7] Therefore, Dijkstra's algorithm uses paths with minimum weight and to help the graph to follow the ICB, there is a need to add a column of nodes with minimal weights (w_{min}) to both sides of the image, which can be removed after segmentation. The following formula shows the weight of the edges which connect adjacent nodes i and j;[7]

$$W_{ij} = 2 - (g_i + g_j) + w_{min} \quad (2)$$

Where:

W_{ij} is the weight assigned to the edge connecting adjacent nodes i and j, $w_{min} = 1 \times 10^{-5}$ is the minimum weight in the graph, and g_i, g_j are the gradient information at node i and j. After calculating the weights maps, to determine the lowest weighted path of a graph between the start and end nodes, Dijkstra's algorithm was used. The obtained path denotes the ICB boundary on the OCT images.[7] An example of the automatic segmentation of ICB is shown in Figure 3.

As mentioned earlier, the automatic detection of OCB is a challenging task, due to the depth of choroidal tissue, which makes this layer to be nonuniform.[7] In this study, the histogram of each OCT image was defined at a particular threshold adaptively based on the mean brightness of each image (the input and output ranges of imadjust function in MATLAB were adaptively defined for each image based on the mean brightness of each image) in another word, by using imadjust function, the range of intensity values for each of the output images decreased adaptively based on the mean brightness of each image (for example; the input and output ranges of imadjust function for the images with the mean brightness of $30 < m < 36$ set to minimum = 0.15 and maximum = 0.20), in which the resulted images became pseudo-binary images (black and white) as shown in Figure 4a. Finally, the pixels with maximum value in each column of the resulting images were found and a third-order curve was assigned to these pixels (using polyfit) that was considered as OCB. Figure 4b shows an example of the automatic segmentation of OCB. Figure 5 shows the block diagram of the proposed method for automatic choroidal segmentation.

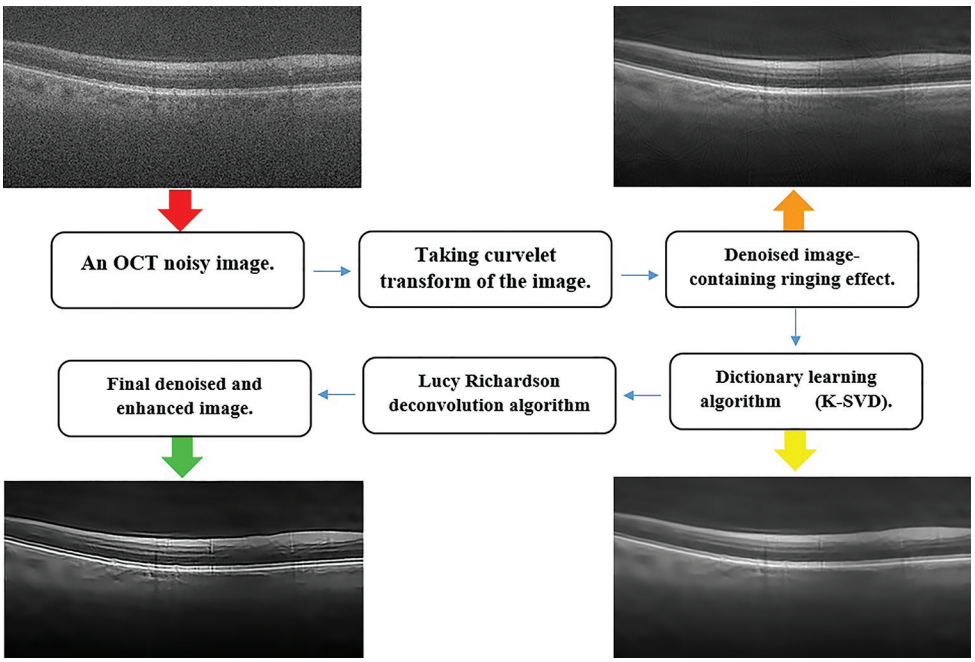

Figure 2: Block diagram of the preprocessing and image enhancement method. OCT - Optical coherence tomography

Results

The proposed preprocessing algorithm was examined on 17 publicly available 2D-OCT images[46] of eyes with and without nonneovascular AMD and 60, 2D EDI-OCT images obtained from Isfahan Feiz Medical Center were utilized to evaluate the proposed automatic choroid segmentation method, also, the brand of OCT machine in this study was Heidelberg Spectralis instrument (Heidelberg Engineering, Heidelberg, Germany). The qualitative performance of our new proposed method on two different OCT images has been illustrated in Figure 6.

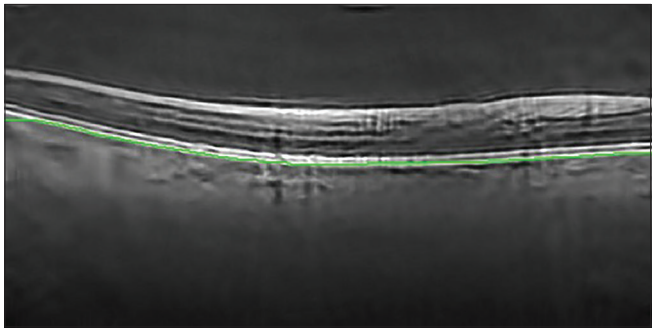

Figure 3: An example of automatic segmentation of ICB, is shown by the green line. ICB - Inner choroidal boundaries

At first, the edge preservation (EP), TP, mean to standard deviation ratio (MSR), contrast to noise ratio (CNR), and equivalent number of looks (ENL) of the performance of our method was calculated for every 17 images. Then, the standard deviation and the mean of the EP, TP, MSR, CNR, and ENL of the performance of our method were compared to the famous denoising techniques [Table 2]. Also, the visual comparison of these different denoising methods is illustrated in Figure 7. When the structures of the image were more flattened and the edges inside the ROI were more blurred, these measurements had smaller

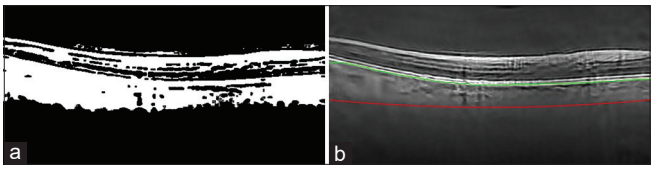

Figure 4: (a) A threshold OCT image, (b) An example of automatic segmentation of OCB, which is shown by the red line, and also the ICB is shown by the green line. OCT: Optical coherence tomography; OCB: Outer choroidal boundary; ICB: Inner choroidal boundary

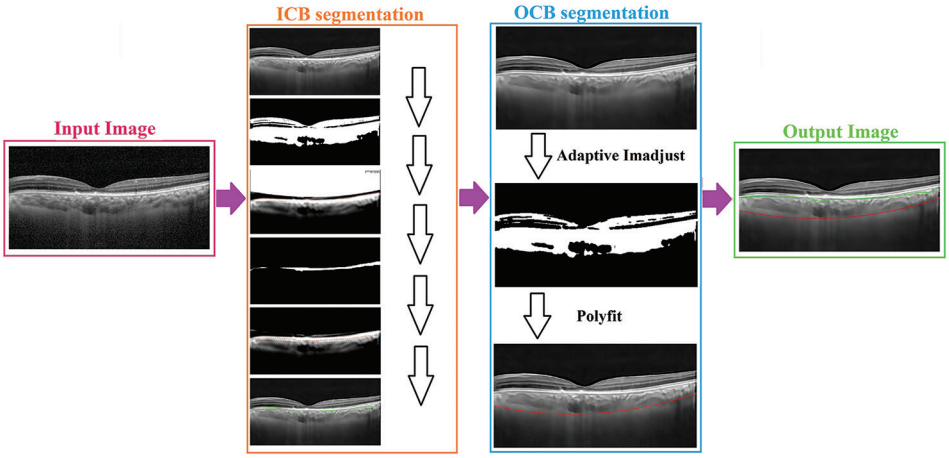

Figure 5: Block diagram of the proposed method for automatic choroidal segmentation. ICB - Inner choroidal boundaries, OCB - Outer choroidal boundaries

Table 2: Mean and standard deviation of the edge preservation, texture preservation, mean to standard deviation ratio, contrast to noise ratio, and equivalent number of look for 17 spectral domain optical coherence tomography retinal images by the use of three dimensional CWDL,[47] Tikhonov,[48] MSBTD,[46] K-SVD,[47] K-SVD based DCUT,[15] and proposed method

	Original	3D CWDL[47]	Tikhonov[48]	MSBTD[46]	K-SVD[47]	K-SVD based DCUT[15]	Proposed method
Mean±STD (EP)[49]	1±0	0.91±0.22	0.71±0.45	0.68±0.59	0.63±0.33	**0.96±0.02**	0.95±0.01
Mean±STD (TP)[49]	1±0	0.41±0.52	0.18±0.85	0.12±0.87	0.32±0.25	0.75±0.05	**0.96±0.02**
Mean±STD (MSR)[50]	3.20±0.46	14.45±4.85	7.64±0.63	14.76±4.75	11.22±2.77	14.36±3.85	**29.33±20.18**
Mean±STD (CNR)[51]	1.27±0.43	7.31±3.63	3.26±0.22	4.76±1.54	4.11±1.23	7.81±3.54	**31.07±19.78**
Mean±STD (ENL)[49]	38.09±4.35	**2323.65±43.54**	74.34±4.32	783.68+67.65	132.01±7.32	1983.08±39.42	69.51±138.12
Mean±STD (PSNR)[52]	-	-	23.67±0.96	**26.46±1.72**	26.13±1.70	17.96±1.08	15.55±1.75

The best result in the table is shown in bold. STD – Standard deviation; EP – Edge preservation; TP – Texture preservation; MSR – Mean to standard deviation ratio; CNR – Contrast to noise ratio; ENL – Equivalent number of look; 3D – Three dimensional; CWDL – Complex Wavelet-based Dictionary Learning; MSBTD – Multi-scale Sparsity-based Tomographic Denoising; K-SVD – K-Singular Value Decomposition; DCUT – Digital Curvelet Transform

values approximate to 0. The TP and EP values in this table demonstrate the ability of our proposed method in preserving the image structures and edges.

At first, the mentioned data consisting of 60 EDI-OCT images were manually segmented by a retinal ophthalmologist, then the automatic segmentation results of the choroid were compared to the manual segmentation applying dice similarity coefficient (DSC). DSC is a statistical metric for comparing the similarity between two samples presented by Thorvald Sørensen and Lee Raymond Dice,[53] respectively in 1948 and 1945. Its formula (given two sets, X and Y) is as the following:

$$\mathrm{DSC} = \frac{2\left|\mathrm{X} \cap \mathrm{Y}\right|}{\left|\mathrm{X}\right| + \left|\mathrm{Y}\right|} \quad (4)$$

The calculated mean DSC for choroidal segmentation of original images (without preprocessing) was 71.99% ± 16.56% and after preprocessing it was 92.14% ± 3.30% for our method, the box-chart of these results is shown in Figure 8. To compare our method with a proposed method by Mazzaferri *et al*.,[17] we implemented their open-source algorithm on our dataset, the mean DSC of their proposed method was calculated as 55.75% ± 14.54%. Figure 9 shows the manual, proposed automatic, and Mazzaferri's automatic segmentation results of the choroid.

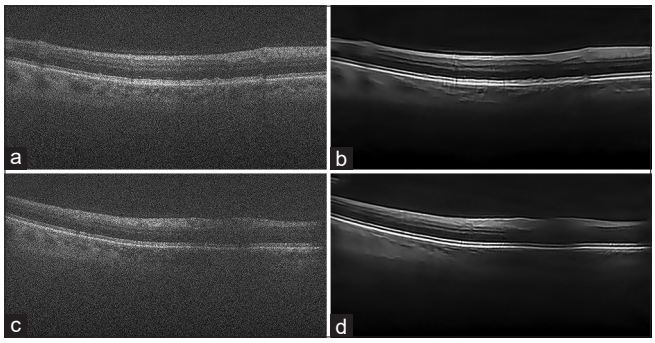

Figure 6: (a) OCT Figure 1 containing speckle noise, (b) Enhanced OCT Figure 1, (c) OCT Figure 2 containing speckle noise, (d) Enhanced OCT Figure 2. OCT - Optical coherence tomography

Discussion

The techniques based on graph searching have been widely used for automatic segmentation of the choroid.[5,7,17,18,20-25,28-32,36,37] In this paper, a new method, based on curvelet transform and graph theory, was implemented for the automatic segmentation of the choroidal layer in OCT B-Scan images. The preprocessing and speckle noise removal of OCT images are important and directly affect the results of automatic segmentation. For this reason, a (2D) curvelet-based K-SVD[15] algorithm was used to suppress the speckle noise and maintain the subtle features of OCT images. Also, due to the unwanted blurring effect of the K-SVD-based denoising method, the resulted images were deblurred by the Lucy–Richardson's deconvolution algorithm[13] and it provided improved output images when compared to the former studies [Table 2] by taking the EP, TP, MSR, CNR, and ENL measures into 17 SD-OCT retinal images. This deconvolution-based method utilized an estimated PSF along with transversal directions. The mean TP, mean EP, mean MSR and mean CNR were increased when compared to five other presented methods. Also, the value of the EP indicated that the proposed, method not only removed the speckle noise but also kept the edges very well. After preprocessing the OCT Images, as described in the methods section, the graph-search-based method was applied to automatic segmentation of the ICB and OCB.

We have compared the manual choroidal segmentation of an expert rater with the results of the proposed automatic segmentation algorithm on OCT images. The agreement between the automatic algorithm and the rater was significant and acceptable. An advantage of the presented method in comparison with other proposed techniques is that our method performed well in both high and low-quality images, but most of the other identical methods

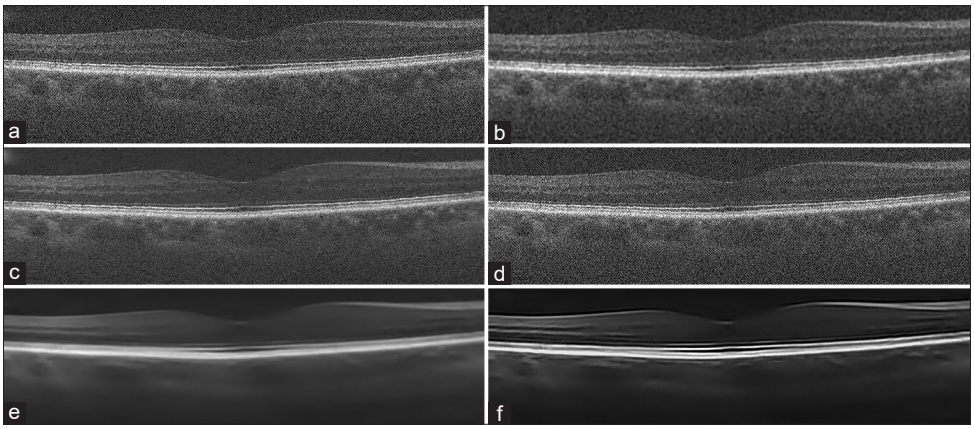

Figure 7: Visual comparison of different denoising methods. (a) The original noisy image; (b) The denoising result using the Tikhonov[48] method; (c) The denoising result using MSBTD[46] method; (d) The denoising result using K-SVD[47] method; (e) The denoising result using K-SVD based DCUT[15] method; (f) Result of the proposed denoising method

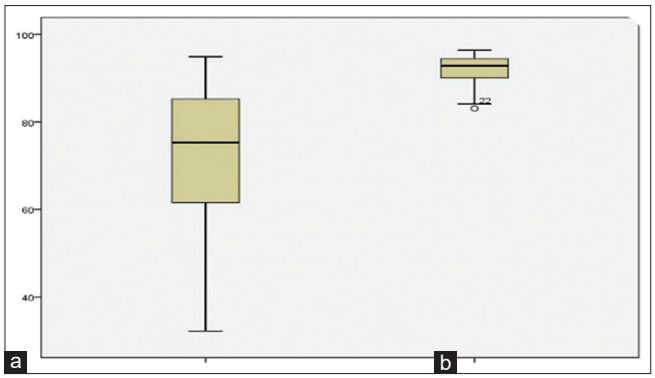

Figure 8: Comparison of choroidal segmentation of (a) original images and (b) the denoised images using the proposed method

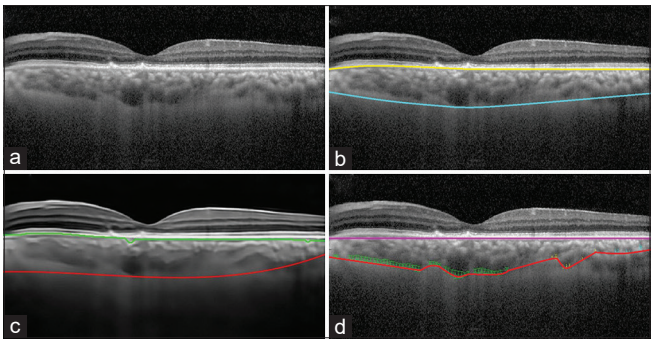

Figure 9: (a) Noisy EDI-OCT image; (b) Manual segmentation of choroidal layer by an expert; (c) Automatic segmentation of choroid by our proposed method; (d) Automatic segmentation of choroid by the use of proposed algorithm by Mazzaferri *et al*.[17] EDI-OCT - Enhanced depth imaging-Optical coherence tomography. The yellow, green, and pink lines show the ICB, while the blue, red, and orange lines represent the OCB. ICB: Inner choroidal boundary; OCB: Outer choroidal boundary

were efficient only in terms of the images with good quality. It was observed that the weak image intensity of OCB and the inhomogeneous intensity of this layer caused less disagreement between the manual and automatic segmentation on some OCT images.

Conclusions

The introduced method in this paper can improve the diagnosis of choroid-related eye diseases. This algorithm is not so complicated and does not need any training; also, it gives precise results even in the presence of high speckle noise. Since our dataset consisted of both normal eyes and eyes with diabetic retinopathy and our method got acceptable results for both of them, this method can be useful in studying the choroid layer in both healthy and diabetic retinopathy eyes on a large scale. Future development of this method will be done by extending the 2D method to 3D and improving the segmentation of this layer and also increasing our dataset.

Acknowledgments

We thank all the patients who participated in this study. Also thanks from Hossein Najafzadeh for useful comments on code programming of the segmentation method.

Financial support and sponsorship

Financial support for this study was provided by a grant from the Research Deputy of Tabriz University of Medical Sciences with grant number 59524. This research did not receive any specific grant from funding agencies in the public, commercial, or not-for-profit sectors.

Conflicts of interest

There are no conflicts of interest.

References

1. Nickla DL, Wallman J. The multifunctional choroid. Progress in retinal and eye research 2010;29:144-68.
2. Wang J, Gao X, Huang W, Wang W, Chen S, Du S, *et al*. Swept-source optical coherence tomography imaging of macular retinal and choroidal structures in healthy eyes. BMC ophthalmology 2015;15:122.
3. Huang W, Wang W, Zhou M, Chen S, Gao X, Fan Q, *et al*. Peripapillary choroidal thickness in healthy Chinese subjects. BMC ophthalmology 2013;13:23.
4. Moussa M, Sabry D, Soliman W. Macular choroidal thickness in normal Egyptians measured by swept source optical coherence tomography. BMC ophthalmology 2016;16:138.
5. Danesh H, Kafieh R, Rabbani H, Hajizadeh F. Segmentation of choroidal boundary in enhanced depth imaging OCTs using a multiresolution texture based modeling in graph cuts. Computational and mathematical methods in medicine 2014; 2014.
6. Behdad B, Rahmani S, Montahaei T, Soheilian R, Soheilian M. Enhanced depth imaging OCT (EDI-OCT) findings in acute phase of sympathetic ophthalmia. International ophthalmology 2015;35:433-9.
7. Alonso-Caneiro D, Read SA, Collins MJ. Automatic segmentation of choroidal thickness in optical coherence tomography. Biomedical Optics Express 2013;4:2795-812.
8. Masood S, Fang R, Li P, Li H, Sheng B, Mathavan A, *et al*. Automatic Choroid Layer Segmentation from Optical Coherence Tomography Images Using Deep Learning. Scientific reports 2019;9:3058.
9. Loupas T, McDicken W, Allan PL. An adaptive weighted median filter for speckle suppression in medical ultrasonic images. IEEE transactions on Circuits and Systems 1989;36:129-35.
10. Portilla J, Strela V, Wainwright MJ, Simoncelli EP, editors. Adaptive Wiener denoising using a Gaussian scale mixture model in the wavelet domain. Image processing, 2001 proceedings 2001 international conference on; 2001: IEEE.
11. George A, Dilienseger J, Weber M, Pechereau A, editors. Optical coherence tomography image processing. Investigative Ophthalmology & Visual Science; 2000: Assoc Research Vision Ophthalmology Inc 9650 Rockville Pike, Bethesda, MD 20814-3998 USA.
12. Herzog A, Boyer KL, Roberts C. Robust extraction of the optic nerve head in optical coherence tomography. Computer Vision and Mathematical Methods in Medical and Biomedical Image Analysis: Springer; 2004. p. 395-407.
13. Koozekanani D, Boyer K, Roberts C. Retinal thickness measurements from optical coherence tomography using a Markov boundary model. IEEE transactions on medical imaging 2001;20:900-16.

14. Ozcan A, Bilenca A, Desjardins AE, Bouma BE, Tearney GJ. Speckle reduction in optical coherence tomography images using digital filtering. JOSA A 2007;24:1901-10.
15. Esmaeili M, Dehnavi AM, Rabbani H, Hajizadeh F. Speckle Noise Reduction in Optical Coherence Tomography Using Two-dimensional Curvelet-based Dictionary Learning. Journal of medical signals and sensors 2017;7:86.
16. Hojjatoleslami S, Avanaki M, Podoleanu AG. Image quality improvement in optical coherence tomography using Lucy–Richardson deconvolution algorithm. Applied optics 2013;52: 5663-70.
17. Mazzaferri J, Beaton L, Hounye G, Sayah DN, Costantino S. Open-source algorithm for automatic choroid segmentation of OCT volume reconstructions. Scientific Reports 2017;7:42112.
18. Kaji V, Esmaeelpour M, Povaay B, Marshall D, Rosin P, Drexler W. Automated choroidal segmentation of 1060 nm OCT in healthy and pathologic eyes using a statistical mode. Biomedical Optics Express 2012;3:86-103.
19. Torzicky T, Pircher M, Zotter S, Bonesi M, Götzinger E, Hitzenberger CK. Automated measurement of choroidal thickness in the human eye by polarization sensitive optical coherence tomography. Optics express 2012;20:7564-74.
20. Tian J, Marziliano P, Baskaran M, Tun TA, Aung T, editors. Automatic measurements of choroidal thickness in EDI-OCT images. Annual International Conference of the IEEE Engineering in Medicine and Biology Society; 2012;2012:5360-3.
21. Zhang L, Lee K, Niemeijer M, Mullins RF, Sonka M, Abramoff MD. Automated segmentation of the choroid from clinical SD-OCT. Investigative ophthalmology & visual science 2012; 53: 7510-9.
22. Hu Z, Wu X, Ouyang Y, Ouyang Y, Sadda SR. Semiautomated Segmentation of the Choroid in Spectral-Domain Optical Coherence Tomography Volume Scans. Investigative Ophthalmology & Visual Science 2013;54:1722-9.
23. Lee S, Fallah N, Forooghian F, Ko A, Pakzad-Vaezi K, Merkur AB, *et al*. Comparative analysis of repeatability of manual and automated choroidal thickness measurements in nonneovascular age-related macular degeneration. Investigative ophthalmology & visual science 2013;54:2864-71.
24. Lu H, Boonarpha N, Kwong MT, Zheng Y, editors. Automated segmentation of the choroid in retinal optical coherence tomography images. 2013 35th Annual International Conference of the IEEE Engineering in Medicine and Biology Society (EMBC); 2013: IEEE.
25. Gerendas BS, Waldstein SM, Simader C, Deak G, Hajnajeeb B, Zhang L, *et al*. Three-dimensional automated choroidal volume assessment on standard spectral-domain optical coherence tomography and correlation with the level of diabetic macular edema. American journal of ophthalmology 2014;158:1039-48. e1.
26. Srinath N, Patil A, Kumar VK, Jana S, Chhablani J, Richhariya A, editors. Automated detection of choroid boundary and vessels in optical coherence tomography images. 2014 36th Annual International Conference of the IEEE Engineering in Medicine and Biology Society; 2014: IEEE.
27. Vupparaboina KK, Nizampatnam S, Chhablani J, Richhariya A, Jana S. Automated estimation of choroidal thickness distribution and volume based on OCT images of posterior visual section. Computerized Medical Imaging and Graphics 2015;46:315-27.
28. Chen Q, Fan W, Niu S, Shi J, Shen H, Yuan S. Automated choroid segmentation based on gradual intensity distance in HD-OCT images. Optics express 2015;23:8974-94.
29. Shi F, Tian B, Zhu W, Xiang D, Zhou L, Xu H, *et al*. Automated choroid segmentation in three-dimensional 1-μm wide-view OCT images with gradient and regional costs. Journal of Biomedical Optics 2016;21:126017.
30. Twa MD, Schulle KL, Chiu SJ, Farsiu S, Berntsen DA. Validation of Macular Choroidal Thickness Measurements from Automated SD-OCT Image Segmentation. Optometry & Vision Science 2016;93:1387-98.
31. Sui X, Zheng Y, Wei B, Bi H, Wu J, Pan X, *et al*. Choroid segmentation from optical coherence tomography with graph-edge weights learned from deep convolutional neural networks. Neurocomputing 2017;237:332-41.
32. Chen Q, Niu S, Fang W, Shuai Y, Fan W, Yuan S, *et al*. Automated choroid segmentation of three-dimensional SD-OCT images by incorporating EDI-OCT images. Computer Methods and Programs in Biomedicine 2017.
33. Al-Bander B, Williams BM, Al-Taee MA, Al-Nuaimy W, Zheng Y, editors. A novel choroid segmentation method for retinal diagnosis using deep learning. 2017 10th International Conference on Developments in eSystems Engineering (DeSE); 2017: IEEE.
34. Chen M, Wang J, Oguz I, VanderBeek BL, Gee JC. Automated segmentation of the choroid in EDI-OCT images with retinal pathology using convolution neural networks. Fetal, Infant and Ophthalmic Medical Image Analysis: Springer; 2017. p. 177-84.
35. Wang C, Wang YX, Li Y. Automatic choroidal layer segmentation using markov random field and level set method. IEEE journal of biomedical and health informatics 2017;21:1694-702.
36. Hussain MA, Bhuiyan A, Ishikawa H, Smith RT, Schuman JS, Kotagiri R. An Automated Method for Choroidal Thickness Measurement from Enhanced Depth Imaging Optical Coherence Tomography Images. Computerized Medical Imaging and Graphics 2018.
37. Salafian B, Kafieh R, Rashno A, Pourazizi M, Sadri S. Automatic segmentation of choroid layer in edi oct images using graph theory in neutrosophic space. arXiv preprint arXiv:181201989 2018.
38. George N, Jiji C. Two stage contour evolution for automatic segmentation of choroid and cornea in OCT images. Biocybernetics and Biomedical Engineering 2019.
39. Eghtedar RA, Esmaeili M, Peyman A, Akhlaghi M, Rasta SH. An Update on Choroidal Layer Segmentation Methods in Optical Coherence Tomography Images: a Review. Journal of Biomedical Physics & Engineering 2022;12:1.
40. Lucy LB. An iterative technique for the rectification of observed distributions. The astronomical journal 1974;79:745.
41. Richardson WH. Bayesian-based iterative method of image restoration. JOSA 1972;62:55-9.
42. Laasmaa M, Vendelin M, Peterson P. Application of regularized Richardson–Lucy algorithm for deconvolution of confocal microscopy images. Journal of microscopy 2011;243:124-40.
43. Starck J-L, Pantin E, Murtagh F. Deconvolution in astronomy: A review. Publications of the Astronomical Society of the Pacific 2002;114:1051.
44. Chiu SJ, Li XT, Nicholas P, Toth CA, Izatt JA, Farsiu S. Automatic segmentation of seven retinal layers in SDOCT images congruent with expert manual segmentation. Optics express 2010;18:19413-28.
45. Dijkstra EW. A note on two problems in connexion with graphs. Numerische mathematik 1959;1:269-71.
46. Fang L, Li S, Nie Q, Izatt JA, Toth CA, Farsiu S. Sparsity based denoising of spectral domain optical coherence tomography images. Biomedical optics express 2012;3:927-42.
47. Kafieh R, Rabbani H, Selesnick I. Three dimensional data-driven multi scale atomic representation of optical coherence

tomography. IEEE transactions on medical imaging 2014;34:1042-62.
48. Sander B, Larsen M, Thrane L, Hougaard JL, Jørgensen TM. Enhanced optical coherence tomography imaging by multiple scan averaging. British Journal of Ophthalmology 2005;89:207-12.
49. Pizurica A, Jovanov L, Huysmans B, Zlokolica V, De Keyser P, Dhaenens F, *et al*. Multiresolution denoising for optical coherence tomography: A review and evaluation. Current Medical Imaging 2008;4:270-84.
50. Cincotti G, Loi G, Pappalardo M. Frequency decomposition and compounding of ultrasound medical images with wavelet packets. IEEE transactions on medical imaging 2001;20:764-71.
51. Bao P, Zhang L. Noise reduction for magnetic resonance images via adaptive multiscale products thresholding. IEEE transactions on medical imaging 2003;22:1089-99.
52. Robinson MD, Toth CA, Lo JY, Farsiu S. Efficient Fourier-wavelet super-resolution. IEEE Transactions on Image Processing 2010;19:2669-81.
53. Dice LR. Measures of the amount of ecologic association between species. Ecology 1945;26:297-302.